Cell Reports, Volume *33*

Supplemental Information

Senescence Induced by BMI1 Inhibition Is a Therapeutic Vulnerability in H3K27M-Mutant DIPG

Ilango Balakrishnan, Etienne Danis, Angela Pierce, Krishna Madhavan, Dong Wang, Nathan Dahl, Bridget Sanford, Diane K. Birks, Nate Davidson, Dennis S. Metselaar, Michaël Hananja Meel, Rakeb Lemma, Andrew Donson, Trinka Vijmasi, Hiroaki Katagi, Ismail Sola, Susan Fosmire, Irina Alimova, Jenna Steiner, Ahmed Gilani, Esther Hulleman, Natalie J. Serkova, Rintaro Hashizume, Cynthia Hawkins, Angel M. Carcaboso, Nalin Gupta, Michelle Monje, Nada Jabado, Kenneth Jones, Nicholas Foreman, Adam Green, Rajeev Vibhakar, and Sujatha Venkataraman

Supplementary Figures and Legends

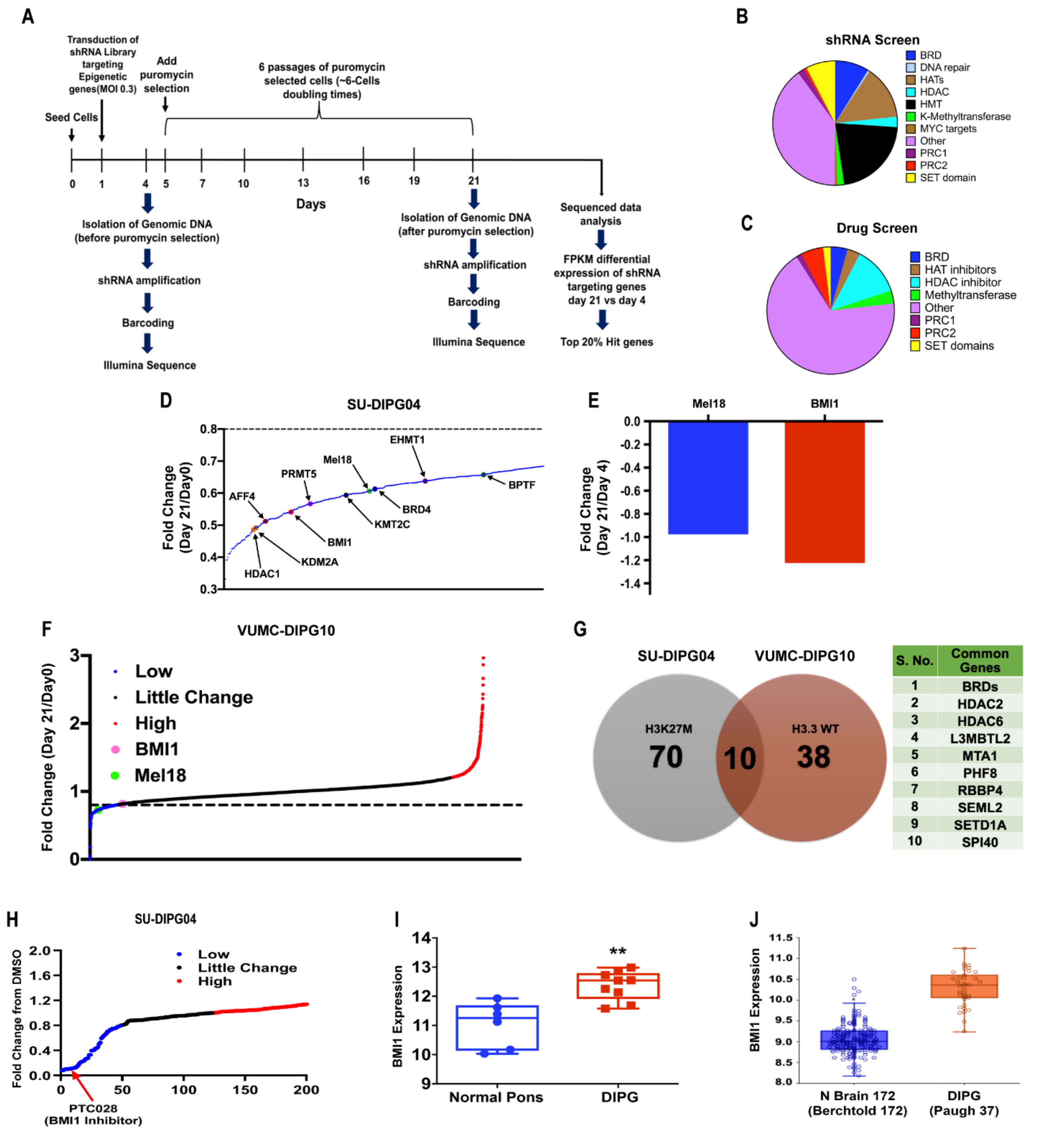

S. No.	Common Genes
1	BRDs
2	HDAC2
3	HDAC6
4	L3MBTL2
5	MTA1
6	PHF8
7	RBBP4
8	SEML2
9	SETD1A
10	SPI40

Figure S1. Epigenetic library screening and target gene evaluation in DIPG cells. Related to Figure 1 and Table S1.

(A) Schematic summary of the method followed in performing the shRNA epigenetic library screening in DIPG. (B and C) A pie chart showing the functional distribution of epigenetic genes in the shRNA pool containing ~408 genes (B) and in the drug screen of small-molecule inhibitors targeting ~ 211 genes

(C). (D) Top-scoring gene hits that positively regulate H3K27M-DIPG cell growth from the primary pooled shRNA screen. (E) The fold-change in Mel18 and BMI1 shRNAs that are significant hits from the shRNA screening. (F) -Fold changes in depleted shRNAs (blue), unchanged shRNAs (black), and enriched shRNAs (red) targeting epigenetic genes from shRNA pool. Blue dots show shRNAs corresponding to the set of genes when knock down inhibits VUMC-DIPG10 (H3 Wt) cell proliferation, black dots represent shRNAs with no change while red dots identify tumor suppressor genes that when inhibited promotes cell proliferation. The x-axis shows shRNA representation for each gene. (G) Venn diagram table showing common gene sets identified by the epigenetic shRNA in SU-DIPG04 (H3K27M) and VUMC-DIPG10 (H3 Wt). (H) Results from the drug screen survival assay with SU-DIPG04 cells using ~211 compounds. The plot shows the –fold change in survival normalized to the vehicle DMSO; with the drugs that inhibit the growth of SU-DIPG04 cells (blue) cause no change (black) and those which induce growth (red). Arrow shows the drug of interest that prominently inhibits the DIPG cell growth greater than 75 percent. (I) Expression of BMI1 in the CHCO cohort of DIPG patient samples from the microarray data; $^{**}p < 0.0014$ DIPG vs. normal. Data represents mean ± SEM. (J) Expression of BMI1 in a larger cohort of DIPG patient samples comparing to its expression in the normal brain regions from the dataset using the R2 genomic data base ($^{****}p$<0.0001). Data represents mean ± SD.

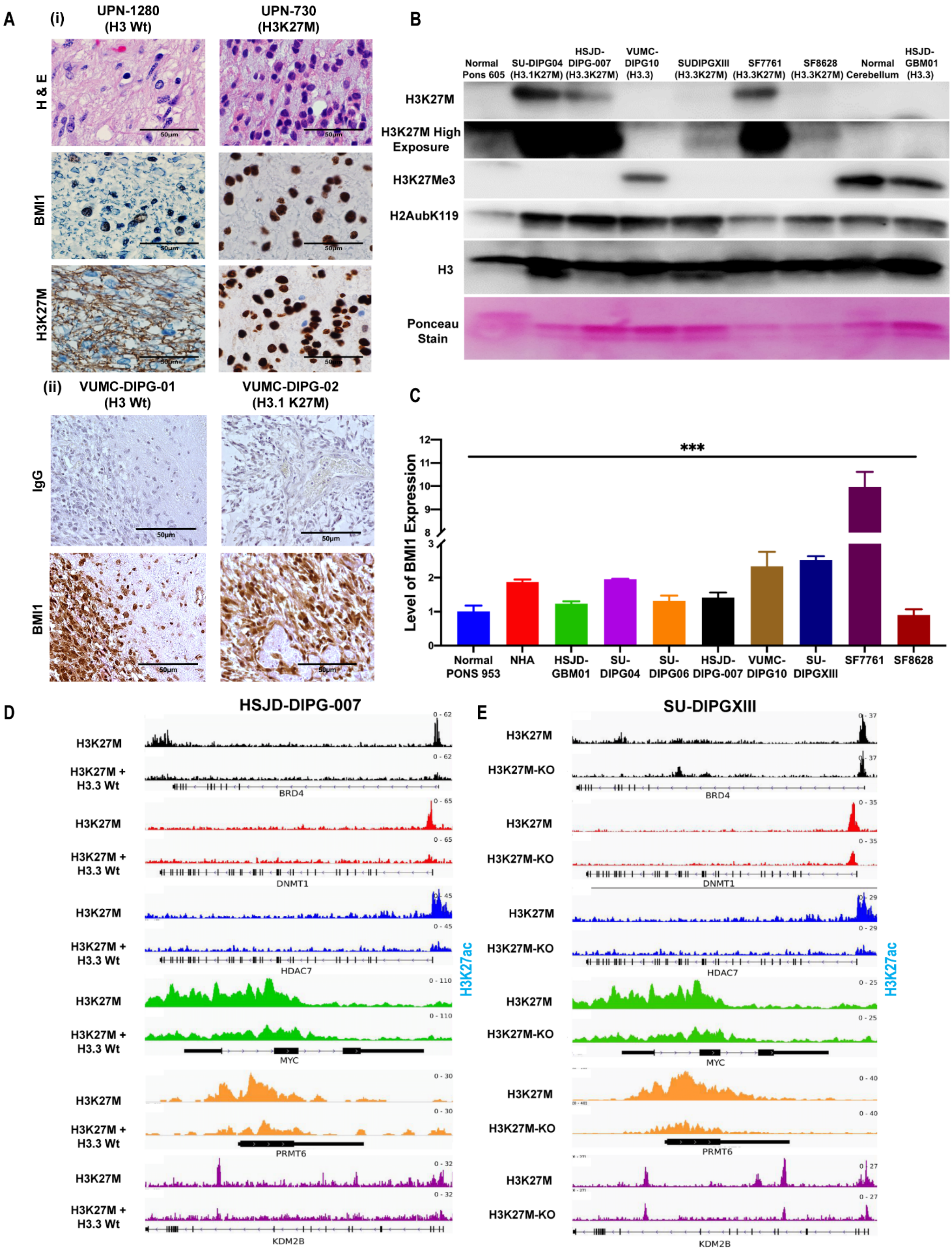

A
(i)
UPN-1280
(H3 Wt)
UPN-730
(H3K27M)
H & E
BMI1
H3K27M
(ii)
VUMC-DIPG-01
(H3 Wt)
VUMC-DIPG-02
(H3.1 K27M)
IgG
BMI1
50µm
B
Normal Pons 605
SU-DIPG04 (H3.1K27M)
HSJD-DIPG-007 (H3.3K27M)
VUMC-DIPG10 (H3.3)
SUDIPGXIII (H3.3K27M)
SF7761 (H3.3K27M)
SF8628 (H3.3K27M)
Normal Cerebellum
HSJD-GBM01 (H3.3)
H3K27M
H3K27M High Exposure
H3K27Me3
H2AubK119
H3
Ponceau Stain
C
Level of BMI1 Expression
***
Normal PONS 953
NHA
HSJD-GBM01
SU-DIPG04
SU-DIPG06
HSJD-DIPG-007
VUMC-DIPG10
SU-DIPGXIII
SF7761
SF8628
D
HSJD-DIPG-007
H3K27M
H3K27M + H3.3 Wt
BRD4
DNMT1
HDAC7
MYC
PRMT6
KDM2B
H3K27ac
E
SU-DIPGXIII
H3K27M
H3K27M-KO

Figure S2: BMI1 and histone expression in DIPG, and changes in H3K27ac enrichment at genomic regions of leading-edge genes (identified in Figure 1F and S1D) in H3 Wt and H3K27M-mutant DIPGs. Related to Figure 2 and 3.

(A) BMI1 expression by IHC in the H3.3 Wt and H3K27M-mutant DIPG patient samples. (i) Samples stained with BMI1 antibody from cell signaling and (ii) samples stained with BMI1 antibody from Novus Biologicals. (B) Expression of indicated histone proteins in normal (Pons, Cerebellum) and brain tumor cell lines (GBM, DIPG). (C) QRT-PCR analysis of BMI1 in normal (Pons, NHA) and brain tumor cell lines (GBM, DIPG) with GAPDH used as an internal control ***$p<0.0001$ (one-way ANOVA) normal vs DIPGs. Data represents mean ± SEM. (D and E) Representative genome tracks comparing H3K27ac localization in the promoter regions of leading-edge genes in parental and H3K27M-mutant modified DIPG lines, HSJD-DIPG-007 cells transduced with H3.3Wt transgene (D) and SU-DIPGXIII cells with H3K27M CRISPR/CAS9 KnockOut (KO) cells (E).

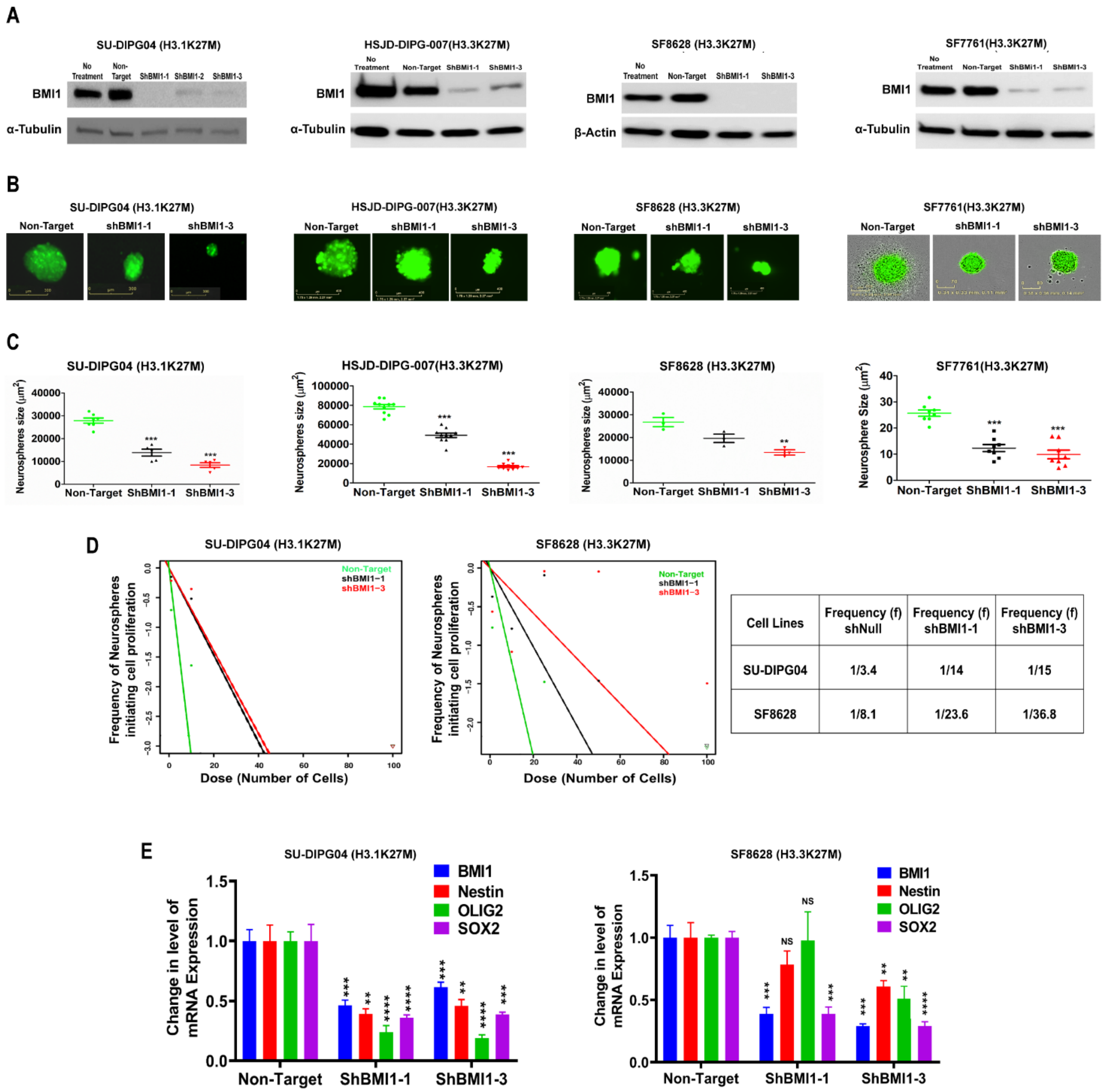

Figure S3. Effect of genetic inhibition of BMI1 on neurosphere formation and cell stemness of H3K27M-mutant DIPG cells. Related to Figure 4.

(A) Western blot showing an effective inhibition of BMI1 in SU-DIPG04, HSJD-DIPG-007, SF8628 and SF7761 using shRNAs targeting BMI1. (B) Representative neurosphere images at day 12 in the above-mentioned cells. (C) Neurospheres formation and quantitation of the neurosphere size as measured and calculated using live-cell imaging system, Incucyte. Using ANOVA, the p-value within the three groups of above four mentioned cell lines are *p<0.0001*, *p<0.0001*, *p<0.005* and *p<0.0001*, respectively. Pair-wise comparisons; ***p<0.004*; ****p<0.0001* shNull vs shBMI1-1 and shBMI1-3 by Student's t-Test. (D) Extreme limiting dilution assay (ELDA) performed using BMI1 knockdown and control non-target SU-DIPG04 and SF8628 cells. Briefly, 1, 10, ….100 cells were seeded on day 1 and the number of spheres formed as measured using Incucyte was counted on day 12 and stem cell frequency was calculated and plotted using ELDA program. Average frequencies are shown in the adjacent table for each condition. (E) QRT-PCR data showing the changes in the stem cell gene expressions upon knockdown of BMI1 using the cells derived from (B). **$p<0.01$; ***$p<0.001$; ****$p<0.0001$ using Student's t-Test. Data represents mean ± SEM.

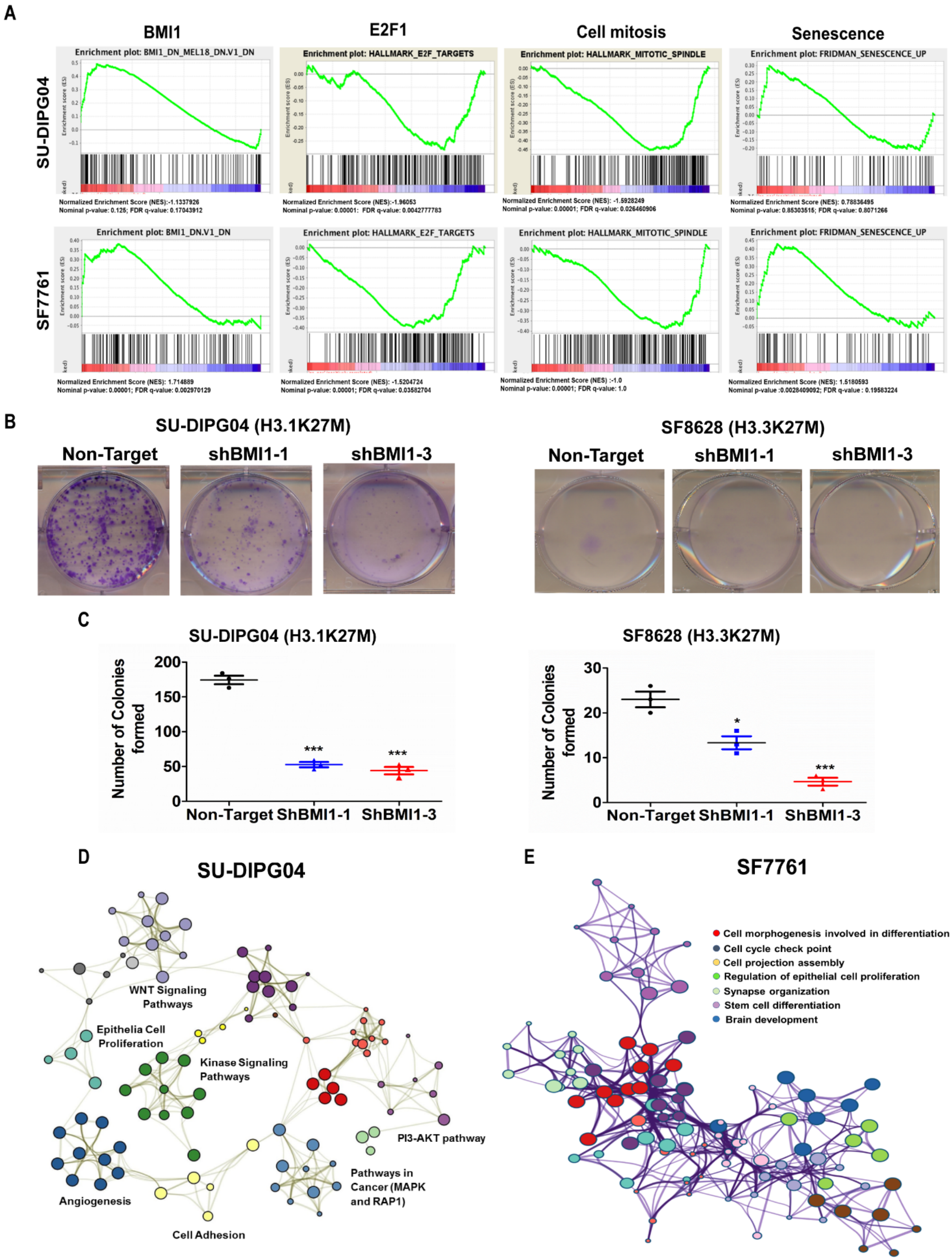

Figure S4. Effect of genetic inhibition of BMI1 on the oncogenic phenotype of H3K27M-mutant DIPG cells. Related to Figure 4.

(A) GSEA analysis of the RNA-Seq data obtained from shBMI-mediated knock down in SU-DIPG04 and SF7761 cells showing significant changes in the gene set specified compared to that of shNull cells; significance threshold set at FDR <0.05. Gene set includes BMI1, E2F1, cell mitosis and senescence. (B) Representative images of the cell colonies formed with the knockdown of BMI1 (n=3). (C) Quantification of colonies forming effect of BMI1 knockdown cells with 2 shRNAs vs shNull. Using ANOVA, the p-value within the three groups for the SU-DIPG04 and SF8628 were $p<0.0001$, and $p<0.0003$, respectively. *$p<0.01$ and ***$p<0.0001$ using Student's t-Test. Data represents mean ± SEM. (D and E) Metascape analysis of differentially expressed genes annotated to functional pathways visualized using Cytoscape visualization software; genes down regulated in SU-DIPG04 shBMI1 (D) and genes upregulated in SF7761 shBMI1(E) compared to those of respective shNull cells.

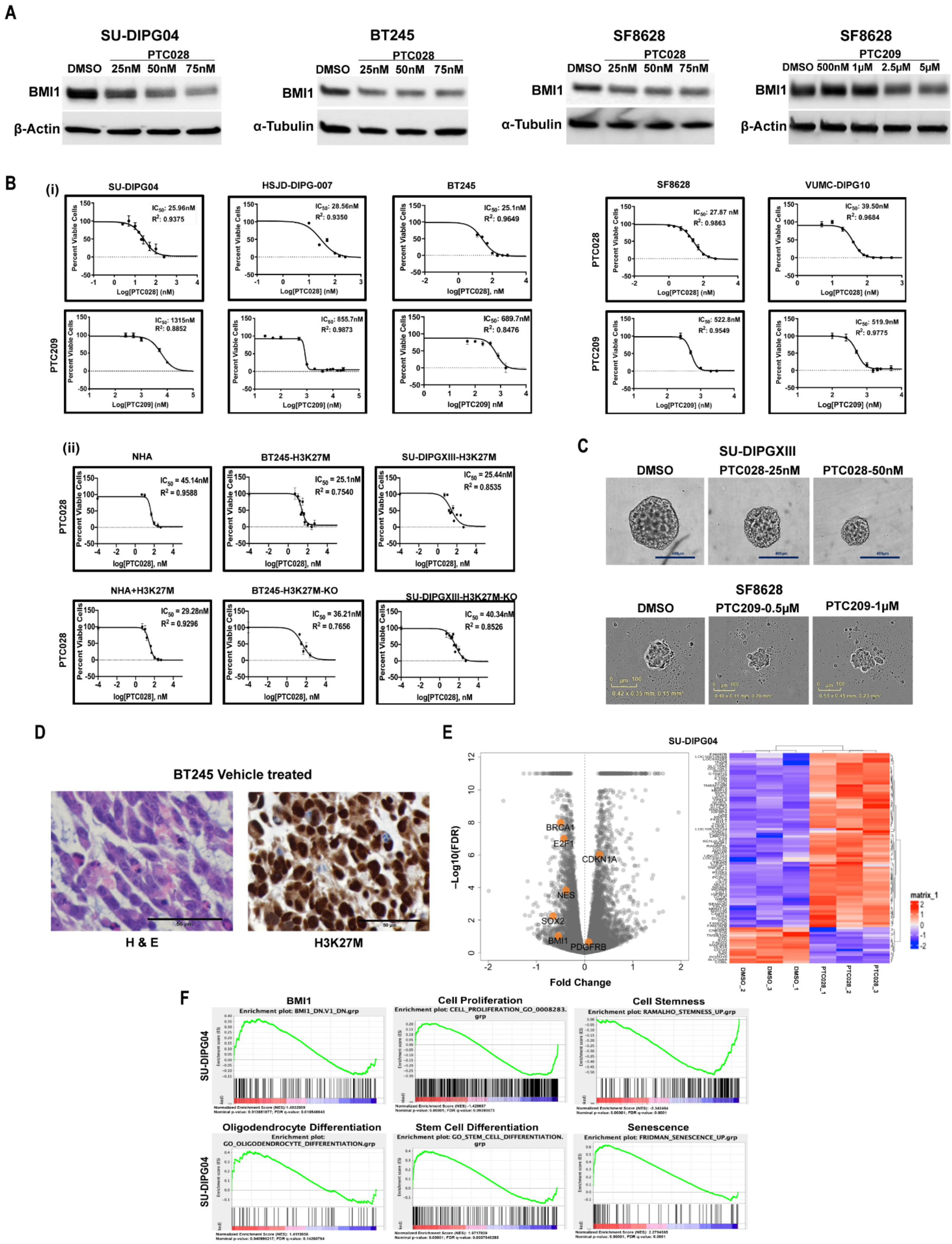
A
SU-DIPG04
PTC028
DMSO 25nM 50nM 75nM
BMI1
β-Actin
BT245
PTC028
DMSO 25nM 50nM 75nM
BMI1
α-Tubulin
SF8628
PTC028
DMSO 25nM 50nM 75nM
BMI1
α-Tubulin
SF8628
PTC209
DMSO 500nM 1μM 2.5μM 5μM
BMI1
β-Actin
B
(i)
SU-DIPG04
HSJD-DIPG-007
BT245
SF8628
VUMC-DIPG10
PTC028
PTC209
Percent Viable Cells
Log[PTC028] (nM)
Log[PTC209] (nM)
IC50: 25.96nM
R2: 0.9375
IC50: 28.56nM
R2: 0.9350
IC50: 25.1nM
R2: 0.9649
IC50: 27.87 nM
R2: 0.9863
IC50: 39.50nM
R2: 0.9684
IC50: 1315nM
R2: 0.8852
IC50: 855.7nM
R2: 0.9873
IC50: 689.7nM
R2: 0.8476
IC50: 522.8nM
R2: 0.9549
IC50: 519.9nM
R2: 0.9775
(ii)
NHA
BT245-H3K27M
SU-DIPGXIII-H3K27M
NHA+H3K27M
BT245-H3K27M-KO
SU-DIPGXIII-H3K27M-KO
log[PTC028], nM
IC50 = 45.14nM
R2 = 0.9588
IC50 = 25.1nM
R2 = 0.7540
IC50 = 25.44nM
R2 = 0.8535
IC50 = 29.28nM
R2 = 0.9296
IC50 = 36.21nM
R2 = 0.7656
IC50 = 40.34nM
R2 = 0.8526
C
SU-DIPGXIII
DMSO
PTC028-25nM
PTC028-50nM
SF8628
DMSO
PTC209-0.5μM
PTC209-1μM
D
BT245 Vehicle treated
H & E
H3K27M
E
SU-DIPG04
−Log10(FDR)
Fold Change
BRCA1
E2F1
CDKN1A
NES
SOX2
BMI1
PDGFRB
matrix_1
DMSO_2
DMSO_3
DMSO_1
PTC028_1
PTC028_2
PTC028_3
F
BMI1
Enrichment plot: BMI1_DN.V1_DN.grp
Cell Proliferation
Enrichment plot: CELL_PROLIFERATION_GO_0008283.grp
Cell Stemness
Enrichment plot: RAMALHO_STEMNESS_UP.grp
Oligodendrocyte Differentiation
Enrichment plot: GO_OLIGODENDROCYTE_DIFFERENTIATION.grp
Stem Cell Differentiation
Enrichment plot: GO_STEM_CELL_DIFFERENTIATION.grp
Senescence
Enrichment plot: FRIDMAN_SENESCENCE_UP.grp
SU-DIPG04

Figure S5: Phenotypic changes in DIPG cells with chemical inhibition of BMI1. Related to Figure 4.

(A) Western blot showing dose dependent decrease in BMI1 protein when DIPG cells were treated with either PTC028 or PTC209 for 5days. (B) (i) Drug-response curves of PTC209 and PTC028 for different DIPG cell lines. (ii) Drug-response curves of PTC028 for the H3K27M-mutant modified NHA and DIPG cell lines. (C) Representative images showing the effect of PTC drugs on cell neurosphere forming ability in DIPG cells. (D) IHC staining of H&E and H3K27M for BT245 xenografts tumor tissue. (E) Volcano plot with heat map adjacent to it showing the changes in genes expressions in SU-DIPG04 cells treated with PTC028 (IC_{50}) compared with DMSO treated cells. Genes highlighted in orange are associated with cell proliferation, stem cell and differentiation pathway genes. (F) GSEA analysis from the RNA-Seq data obtained from SU-DIPG04 cells treated with PTC028 (IC_{50}) compared to DMSO treated cells annotated to multiple signaling pathway gene sets.

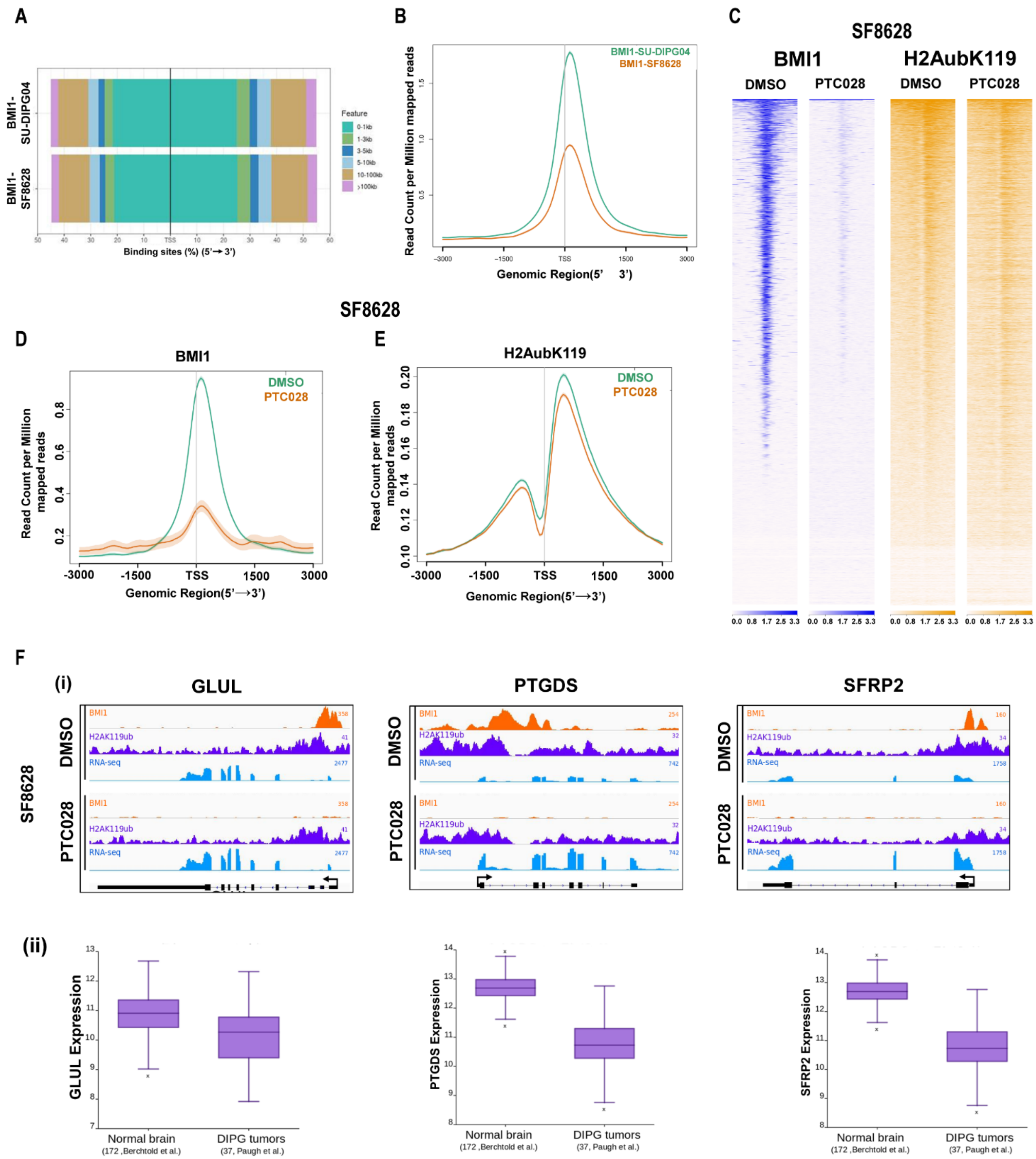

Figure S6. Changes in BMI1 and H2AubK119 occupancy at different gene loci and the corresponding changes in their gene expression level with PTC028 treatment in DIPG cell lines. Related to Figure 5.

(A) Distribution of BMI1 peaks relative to TSS in SU-DIPG04 and SF8628 cells. (B) Average profiles of BMI1 peaks relative to TSS (±3kb) in SU-DIPG04 (green) and SF8628 (orange) cells. (C) ChIP-Seq heat maps of BMI1 (blue) and H2AubK119 (orange) in SF8628 cells treated with DMSO or PTC028 at regions surrounding ±3kb relative to the TSS. (D) Average profiles of BMI1 peaks relative to TSS (±3kb) in SF8628 cells treated with DMSO (green) or PTC028 (orange). (E) Average profiles of H2AubK119 peaks relative to TSS (±3kb) in SF8628 cells treated with DMSO (green) or PTC028 (orange). (F)(i) Genome browser views representing the results of ChIP-Seq for BMI1 and H2AubK119 for the genes GLUL, PTGDS and SFRP2 and their changes with PTC028 treatment in the SF8628 cells. The changes in the gene transcription are shown in the RNA-seq tracks below. (ii) Boxplots representing the mRNA expression levels of these genes in normal brain tissues and in primary DIPG tumors collected from the R2 genomic data base; ****p<0.0001; (Berchtold et al., 2008; Paugh et al., 2011). Data represents mean ± SD. NS= non-significant.

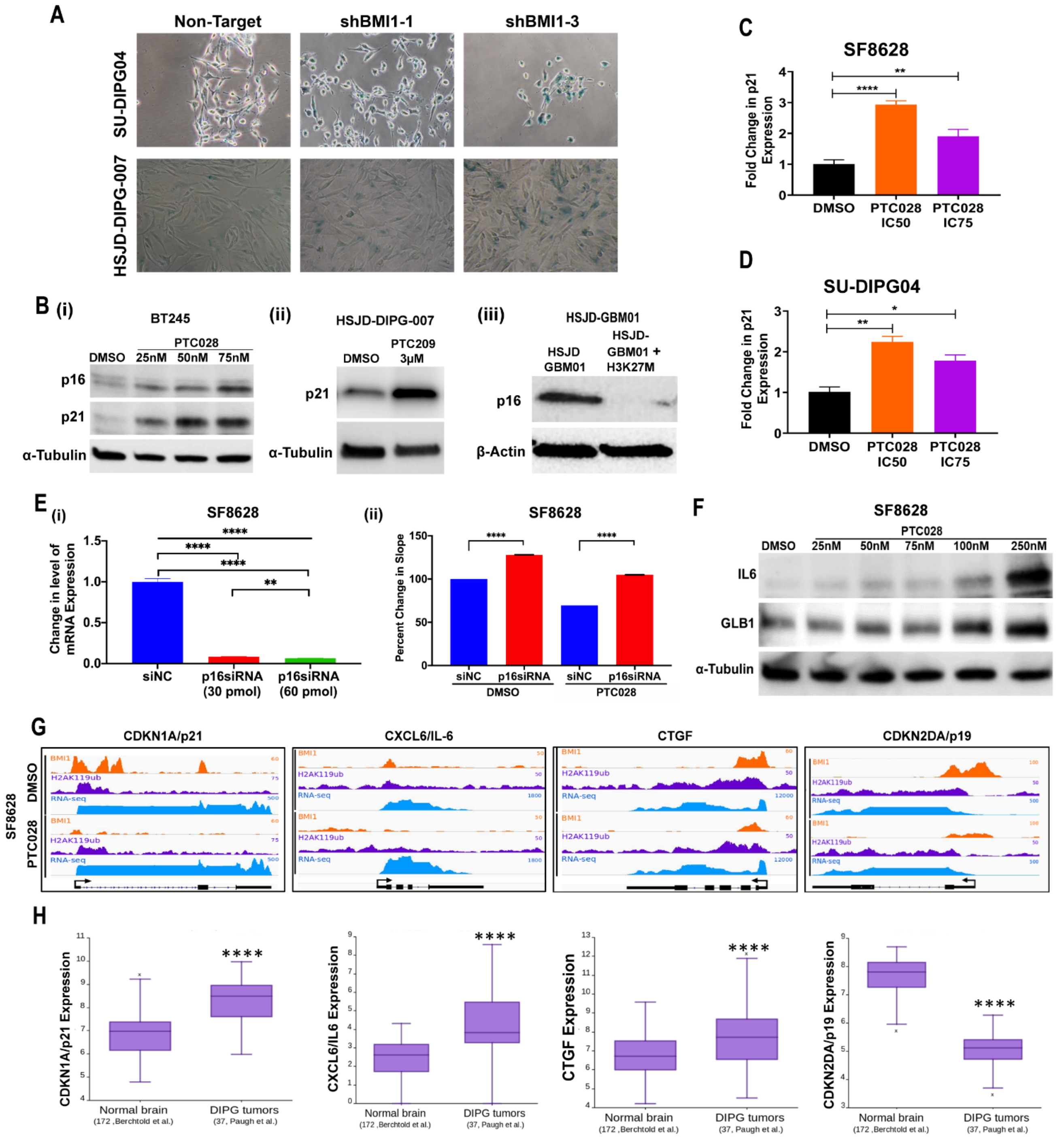

Figure S7. Induction of senescence and senescence associated gene markers with genetic and pharmacological inhibition of BMI1 in DIPG cells. Related to Figure 6.

(A) Representative images of Senescence Associated β-Galactosidase (SA-β-gal) staining in SU-DIPG04 and HSJD-DIPG-007 cells with knockdown of BMI1. (B) Representative western blot analysis of different senescent proteins mentioned in BT245, HSJD-DIPG-007 and HSJD-GMB01 cells. (C and D) -Fold increase in p21 mRNA expression with PTC028 treatments as measured by QRT-PCR in SF8628 (C) and SU-DIPG04 (D). (E) Changes after 72hrs of transfection with siRNA directed to p16 in SF8628 cells in: (i) p16 mRNA expression and (ii) cell proliferation rate with PTC028 treatment. By ANOVA, ****$p<0.0001$. Pair-wise comparison, **$p<0.01$ and ****$p<0.0001$ *by* Student's t-test. (F) Western blot of IL6 and GLB1 after 5 days with PTC028 treatment in SF8628 cells. (G) Genome browser views representing the results from the BMI1 and H2AubK119 ChIP-Seq peaks along with the transcriptomic expression from the RNA-Seq data for CDKN1A, CXCL6, CTGF and CDKN2D in SF8628 cells with PTC028 or DMSO treatments. (H) Boxplots representing the respective mRNA expression levels obtained using the R2 genomic data base for normal brain tissues and in primary DIPG tumors; ****p<0.0001 (Berchtold et al., 2008; Paugh et al., 2011). Data represents mean ±SD.

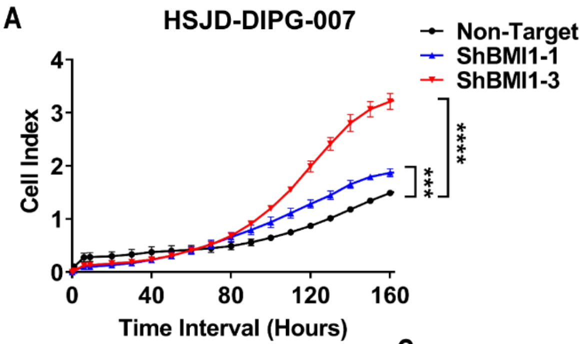

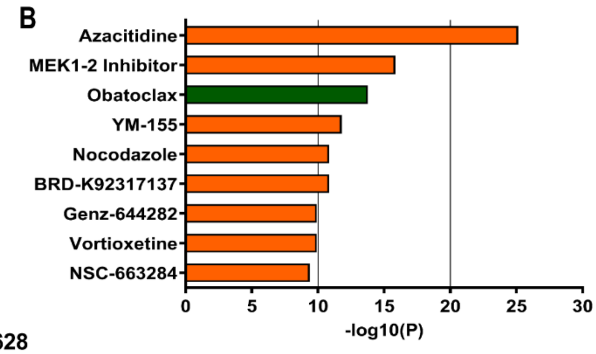

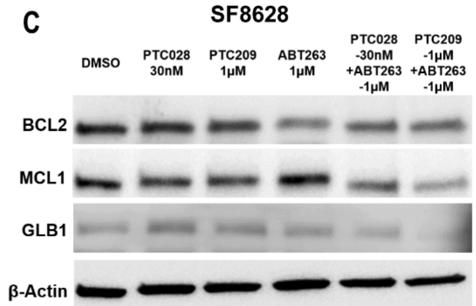

D

SF8628

	PTC028 5nM	PTC028 10nM	PTC028 25nM	PTC028 50nM
ABT263 100 nM	10.79	2.64	0.89	0.27
ABT263 250 nM	2.07	1.74	0.37	0.11
ABT263 500 nM	1.21	0.97	0.22	0.04
ABT263 1000 nM	1.06	0.90	0.24	0.02

SU-DIPG04

	PTC028 5nM	PTC028 10nM	PTC028 25nM	PTC028 50nM	PTC028 75nM
ABT263 0.1uM	0.24	0.25	0.40	0.76	1.18
ABT263 0.25uM	0.23	0.24	0.37	0.72	1.11
ABT263 0.5uM	0.26	0.26	0.37	0.76	1.14
ABT263 1uM	0.23	0.22	0.35	0.65	0.99
ABT263 2uM	0.09	0.15	0.33	0.61	0.96

CI=1 ADDITIVE
CI<1 SYNERGY
CI>1 ANTAGONISTIC

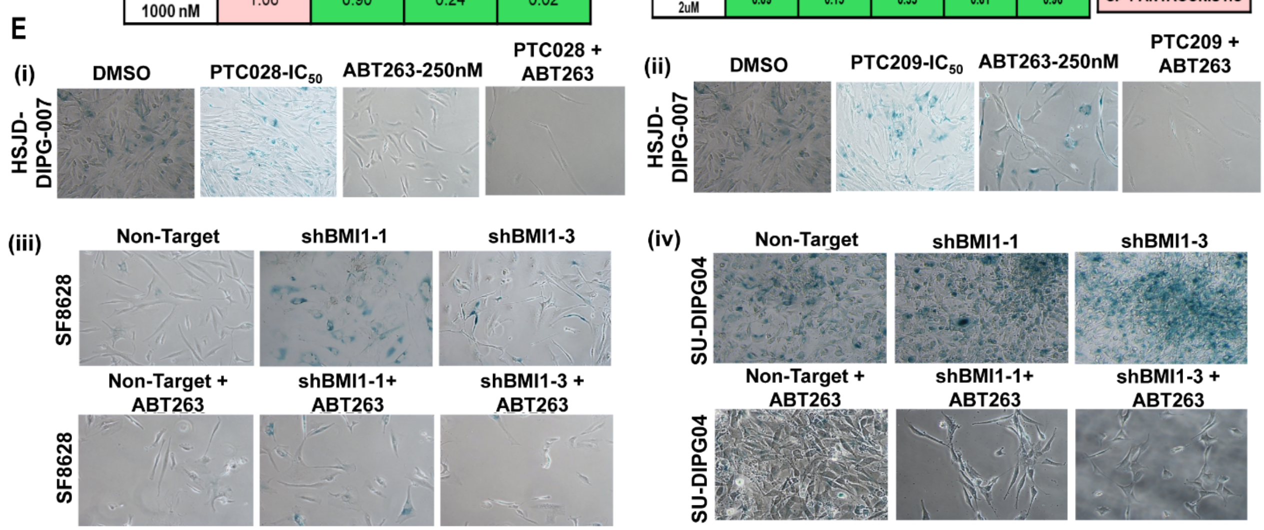

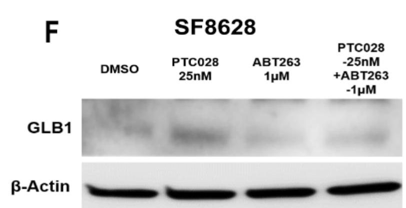

Figure S8. Removal of senescent cells using BH3 mimetics enhances the anti-tumor effect of BMI1 inhibitor *in vitro*. Related to Figure 6.

(A) Cell proliferation index of HSJD-DIPG-007 cells as measured in real-time using XCELLigence in the genetic BMI1 knockdown and shNull cells, both cultured long-term. ***$p<0.0003$; ****$p<0.0001$ using Student's t-Test. (B) Meta-analysis, using the Metascape suite of tools depicting top predicted synthetic lethal compounds that are synergistic with PTC028 in DIPG cell killing. Input gene lists were the significantly enriched genes after PTC028 treatment relative to DMSO treatment in SF8628 and SU-DIPG04 by RNA-seq. One of the top agents identified in green is Obatoclax, a BH3 mimetic. (C) Western blot showing the changes in the BH3 proteins and senescence marker GLB1 in SF8628 cells sequentially treated with PTC compounds and ABT263. (D) Representative MTS assay read out showing synergistic cell killing effect of PTC028 and ABT263 as measured by combination indices calculated based on Chou and Talalay theorem. (E) Representative pictures of SA-β-gal staining of DIPG cells with different treatment conditions shown. (F) Western blot showing the changes in GLB1 protein expression in SF8628 treated with PTC028 and ABT263.

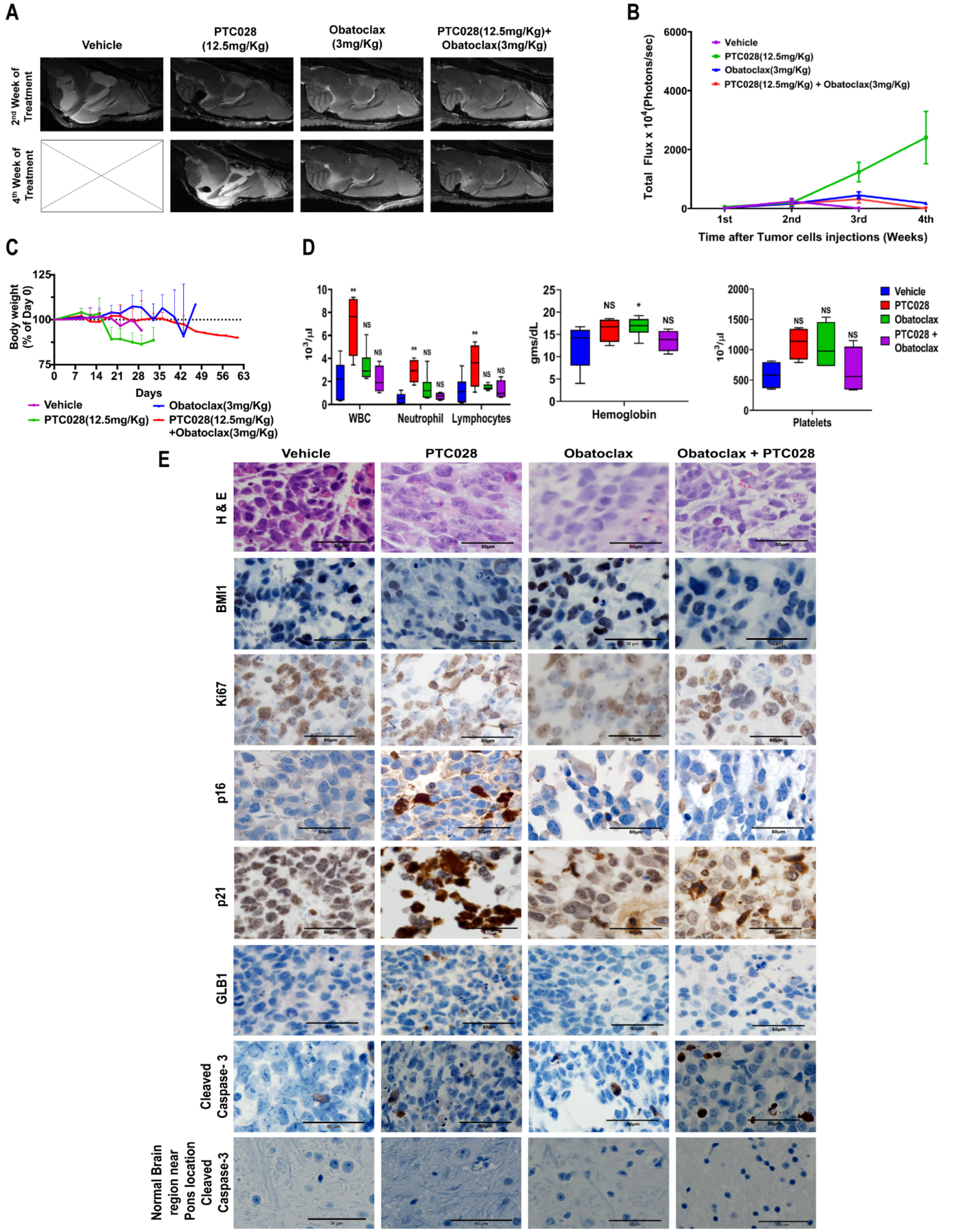

Figure S9: Analysis of the *in vivo* anti-tumor and toxicity effects of PTC028, Obatoclax and their combination treatments. Related to Figure 7.

(A) Representative sagittal MRI images of the intracranial pons tumor, taken at the 2nd week of treatments and at the 4th week (one week after the treatments were stopped). (B) Statistical analysis of the bioluminescence total flux intensity of the pons tumor every week till 4th week during the study. Data represents mean ± SEM. (C) The percentage change in the mouse body weight from day 0 measured throughout the course of different treatments. Data represents mean ± SEM. (D) Complete blood count (CBC) analysis from the blood collected immediately after animals were euthanized upon reaching their end point. Samples were analyzed for WBC (leukocyte), hemoglobin (Hb), neutrophils, lymphocytes and platelets count. Data represents mean ± SEM. (E) Residual tumors are harvested at the end points of the animal subjected to different treatments, fixed and stained for H & E, BMI1, Ki67, p16, p21, GLB1 and cleaved caspase 3 along with cleaved caspase 3 protein tested in the normal regions of the brain next to the tumor site.